García Martínez, A.; Monsalve-Serrano, J.; Lago-Sari, R.; Dimitrakopoulos, N.; Turnér, M.; Tunestål, P. (2019). Performance and emissions of a series hybrid vehicle powered by a gasoline partially premixed combustion engine. Applied Thermal Engineering. 150:564-575. https://doi.org/10.1016/j.applthermaleng.2019.01.035

Performance and emissions of a series hybrid vehicle powered by a gasoline partially premixed combustion engine

Antonio García[a,*], Javier Monsalve-Serrano[a], Rafael Sari[a], Nikolaos Dimitrakopoulos[b], Martin Tunér[b], Per Tunestål[b]

a- CMT - Motores Térmicos, Universitat Politècnica de València, Camino de Vera s/n, 46022 Valencia, Spain
b- Department of Energy Sciences, Lund University, Ole Römers Väg 1, 22363 Lund, Sweden

Applied Thermal Engineering
Volume 150, 5 March 2019, Pages 564-575

Corresponding author (*):
Dr. Antonio García Martínez (angarma8@mot.upv.es)
Phone: +34 963876574
Fax: +34 963876574

Abstract

This work evaluates the performance and emissions of the series hybrid vehicle concept powered by a gasoline partially premixed internal combustion engine. To do so, experimental data was collected from a Volvo VED-D4 Euro 6 four-cylinder compression ignition engine running under gasoline partially premixed combustion. Two series hybrid vehicle models were developed in GT-Power®, which were fed with the experimental data to evaluate the potential of the hybrid concept. First of all, the battery charging strategy of the hybrid vehicles was optimized in terms of number of power levels and operating conditions. For this, a design of experiments was performed in GT-Power®, which enabled to obtain a predictive model of the performance and emissions. The predictive model was used to obtain the optimized NOx-fuel consumption Pareto frontiers for each charging strategy proposed. Finally, the GT-Power® vehicle models were run with the optimal operating conditions (selected from each Pareto) in both the new European driving cycle and worldwide harmonized light vehicles test cycle. The results show that the hybrid powertrain running with partially premixed combustion is able to achieve similar or better performance than the commercial diesel vehicle with low engine-out emissions. Moreover, comparing the results from both vehicles, it was confirmed that the hybridization results in better improvements when applied to urban traffic than for highway conditions where the power request is higher and the potential for regenerative braking is reduced.

Keywords

Low temperature combustion; series hybrid vehicle; emissions; worldwide harmonized light vehicles test cycle

1. Introduction

Internal combustion engines (ICE) still stands as the major propulsion system for transportation, being found from small applications to high power generation as the

ones in ships and power plants [1]. Despite of the increasing number of alternative fuels as ethanol, butanol, dimethyl ether (DME), etc., it is expected that even by 2040 ICEs running with petroleum-based fuels will deliver approximately 90% of the total energy in the transportation sector [2]. The high efficiency of diesel compression ignition engines placed them in the lead of the usage in transportation sector. In spite of this, the high NO_x and soot emissions produced during the diesel combustion process became subject of social concern due to the health issues than can be unleashed by these pollutants [3]. Therefore, stringent regulations were developed to avoid the air contamination, forcing the original equipment manufacturers (OEM) to develop systems that allow reducing the tailpipe emissions from the engines [4]. As consequence, nowadays vehicles are equipped with three main aftertreatment systems. The selective catalyst reduction (SCR) system relies on using urea injection to convert NO_x emissions to N_2. Additionally, the diesel particulate filter (DPF) removes the soot content in the exhaust gas whilst the diesel oxidation catalyst (DOC) oxidizes the hydrocarbons (HC) and carbon monoxide (CO) emissions [5] and improves the passive soot oxidation in the DPF through the NO_2 generation [6]. However, the addition of these subsystems increases the final vehicle complexity and cost, important factors for the final consumer. Thus, alternative combustion concepts started to be investigated aiming to achieve diesel-like efficiency with reduced engine-out emissions.

In this scenario, the low temperature combustion (LTC) concepts demonstrate the capability of achieving high efficiency values while avoiding the NOx-soot trade-off [7]. Generally, the LTC combustion occurs in a highly exhaust gas recirculation (EGR) diluted environment, that allows a fast combustion process, with reduced heat transfer [8]. The first developed premixed LTC strategy is the homogeneous charge compression ignition (HCCI). This strategy relies on a very early fuel injection timing, allowing to obtain a homogeneous charge mixed with high amounts of EGR prior the combustion process [9].The compression stroke increases the temperature and pressure inside the chamber, reaching an auto ignition condition in several combustion chamber points. This leads to a rapid combustion process, with reduced time for heat transfer, leading to thermal efficiency values higher than conventional diesel combustion (CDC) [10]. It was also demonstrated that this combination of factors allows to achieve virtually zero NOx and soot emissions [11]. Nonetheless, intrinsic drawbacks complicates the implementation of this combustion concept. The controllability over this combustion process is reduced since the combustion start is driven by chemical kinetics [12]. In this sense, as the engine load is increased, the combustion process starts early in the compression stroke leading to excessive pressure gradients and consequently mechanical fatigue limiting the maximum load that can be achieved. Moreover, it is difficult to obtain a stable operation at low engine loads causing higher amount of HC and CO generated as function of the poor combustion efficiency [13].

A widely addressed LTC combustion strategy nowadays is the so-called reactivity controlled compression ignition (RCCI), which relies on using two fuels of different reactivity to obtain control of the combustion process. The basis of this combustion mode has its roots in the work by Inagaki et al. [14], where they proposed a dual-fuel premixed compression ignition (PCI) combustion strategy using two fuels with different reactivity. In this concept, the fuels are injected into the cylinder using two separate injection systems, allowing the variation of each fuel independently according to the

engine operating conditions [15]. By means of experimental tests, the authors confirmed better combustion controllability than HCCI with low NOx and soot emissions. The most common LRF and HRF fuels used to implement the RCCI concept are diesel and gasoline because of their availability in the market [16], but this concept was proved to be able to run with several other alternative fuels [17][18][19]. The main advantage of this combustion concept is the capability to change the mixture reactivity according to the engine condition allowing to obtain simultaneous NOx, Soot and higher conversion efficiency [20]. The LRF quantity should be low at low engine loads to improve the combustion efficiency. As the engine load is increased towards medium load conditions, the LRF amount is also increased. At high loads, the LRF portion must be moderated to avoid excessive pressure rise rate (PRR) and maximum in-cylinder pressures [21]. Several works demonstrate that RCCI is capable of reaching the steady-state NOx and soot levels imposed by the EURO VI regulation without aftertreatment necessities under different engine platforms [22][23][24]. Additionally, studies demonstrates that the amounts of HC and CO generated during RCCI operation can be reduced to EURO VI levels with the increase of the DOC volume or taking advantage of the thermal inertia during the engine operation [25][26][27]. However, the necessity of using two fuels stored in separate tanks is a major drawback for the implementation of the RCCI concept in light-duty vehicles.

Another promising LTC concept nowadays together with RCCI is the gasoline partially premixed combustion (PPC). The literature demonstrates that the use of gasoline fuel in the PPC mode extends the ignition delay and allows better control of the combustion process than HCCI as load increases [28]. Moreover, recent studies performed on a light-duty Euro 6 diesel engine running under gasoline PPC demonstrated that it is possible to obtain better fuel consumption than CDC while reducing NOx and soot levels up to 50% [29]. Using conversion factors to relate the steady-state emissions to transient conditions, it was possible to verify that the final NEDC results for NOx were closer to Euro 6 constraints [30]. Thus, since it is a single-fuel LTC concept, and non-dependent on diesel fuel, it could have a greater acceptance and need lower investment for its application than RCCI. One drawback with gasoline PPC is the operation at low load, which was found to be compromised when gasoline fuels with octane number (ON) higher than 91 are used [31]. The use of a spark plug to control the combustion process at low load was found to be a possible alternative [32]. However, the benefits in terms of NOx and soot emissions that characterize the LTC concepts disappeared due to the need of rich local equivalence ratios between the spark plug electrodes [33]. Thus, it is clear that one possibility to exploit the benefits of the gasoline PPC concept should be to use it inside a multi-mode operation, which would lead to work in the most efficient part of the engine map for the concept [34].

Despite of the advances in the combustion area, future CO_2 levels imposed by the emissions regulations will be still a challenge to be overcome by the OEMs. The electrification and hybridization are paths that have been used by the manufacturers due to the possibility to reduce the total CO_2 emitted by the fleet [35]. In both paths, the ICE engine still plays a major role as power generator, being responsible for charging the batteries and providing additional power to the wheels depending on the hybrid concept. Series hybrids are known as the more efficient concept due to the lower mechanical losses in the energy path. In this case, the ICE is used as a range extender,

providing the energy required to recharge the batteries according to a predefined strategy. The parallel concept relies on using the ICE for battery charging and for vehicle traction. In this case, the engine is connected to the gearbox, delivering extra power to reach high power demands. In these hybrid applications, the ICE are typically operated under conventional combustion modes (i.e., spark ignition or conventional diesel combustion). However, the LTC concepts could be also an attractive solution due to its high efficiency with reduced engine-out emissions.

Therefore, the objective of the current work is to evaluate the potential of the gasoline PPC concept applied in a series hybrid vehicle in order to assess its possible advantages compared to conventional diesel powertrains. The experimental maps obtained for the Volvo VED-D4 Euro 6 four-cylinder compression ignition engine running under gasoline partially premixed combustion were used as inputs for two different vehicles models developed in GT-Power® (Volvo XC90 and Volvo V60). This allows to assess the hybridization potential on two vehicles of different category. The new European driving cycle (NEDC) and worldwide harmonized light vehicles test cycle (WLTC) were used to assess the performance and emission results and compare to the manufacturer data. Prior to the final comparison, a detailed optimization study was carried out to obtain the best ICE operating conditions to charge the batteries for each driving cycle and vehicle.

2. Materials and methods

2.1. Engine, test cell and fuel

The engine used in this experimental campaign is a Volvo VED-D4 Euro 6 four-cylinder engine. The engine is equipped with a conventional diesel common rail injection system and a standard two-stage turbocharger. A scheme of the test engine setup is shown in Figure 1, and the main engine specifications are reported in Table 1. As shown in Figure 1, the engine is not equipped with aftertreatment systems, so that all the reported emissions are engine-out.

The base engine has been modified to add a low-pressure EGR system, an air heater before the compressor and four cylinder pressure transducers in the place of the glow plugs. Apart from that, the engine is equipped with pressure transducers and thermocouples in several positions from the intake to the exhaust line. The in-cylinder pressure is measured using a Kistler piezoelectric transducer (range 0-200 bar) and acquired using the AVL-Indismart device. The pressure signals are averaged over 150 consecutive cycles, and the apparent heat release (HR) and heat release rate (HRR) are calculated using the equations reported by Heywood [36].

All engine calibration parameters (injection, EGR valve position, VGT position, etc.,), pressure, temperature signals and pollutant emissions are acquired and controlled using a PXI-National Instrument device with an in-house program developed in LabView software.

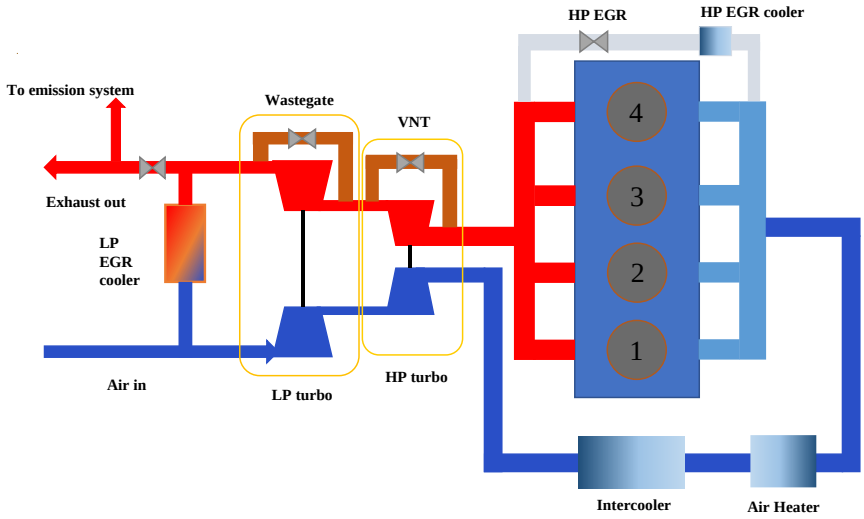

Figure 1. Engine layout.

Table 1. Engine characteristics.

Engine Type	Volvo VED-D4 two-stage turbocharger Euro 6
Number of cylinders [-]	4
Displaced volume [cm^3]	1969
Stroke [mm]	93.2
Bore [mm]	82
Compression ratio [-]	15.8:1
Valves/cylinder [-]	4
Rated power [kW]	168 @ 4250 rpm
Rated torque [Nm]	470 @ 1750-2500 rpm
Injection system [-]	Common rail (max inj. Pressure=2500 bar)
Injector and nozzle [-]	Solenoid 8 holes

The fuel used in this work is gasoline supplied by Chevron, with 75 research octane number (RON) and 68 motor octane number (MON). The gasoline has sufficient lubricity to preserve the fuel injection system from damage. The fuels characteristics are listed in Table 2. The selected low octane number gasoline (RON 75) with respect to the commercial gasoline adopted in a spark ignition engine (RON> 90), is selected from a previous study that highlights the possibility to extend the PPC load range [37].

Table 2. Fuel properties.

	Gasoline
RON [-]	75
MON [-]	68
H/C [-]	2.02
Lower heating value [MJ/kg]	43
A/F stoich [-]	14.9

2.2. Vehicles, computational model and driving cycles

The vehicles selected to perform the simulations are the Volvo XC90 and Volvo V60, which equip the diesel engine used in the experimental tests. The vehicles have been selected because they belong to different car families, SUV (XC90) and estate (V60), and therefore they have substantially different characteristics, as shown in Table 3. The electrical components shown in Table 3 have been defined and added to the vehicle to perform the study, while the other specifications come from the manufacturer data [38][39].

Table 3. Vehicles specifications.

Vehicle [-]	Volvo V60	Volvo XC90
Vehicle Mass [kg]	1824	2434
Vehicle Drag Coefficient [-]	0.29	0.33
Frontal Area [m²]	2.23	2.78
Tires Size [mm/%/inch]	215/55/R16	235/55/R19
Vehicle Wheelbase [m]	2.776	2.984
Final Drive Ratio [-]	3.88	3.33
Electric motor power [kW]	50	60
Generator power [kW]	30	35
Battery Size [Ah]	32	45
Battery component [-]	Li-ion	Li-ion

Both vehicles have been modeled in GT- Power® following the data provided in the OEM website. Figure 2 illustrates the model developed for the V60 with the respective sub-assemblies that stands for the different vehicle systems. As it can be seen, the model consists of several sub models as the “VEHICLE” where the majority of the geometric characteristics are defined, “ICE” and the supervisory controller that is responsible to control the SOC and the engine state. Additionally, the electric motors are represented by “GEN” (generator) and “TM” (traction motor). The time speeds profiles are defined in the object “DRIVER”, which consists of a PID controller that determine the instantaneous required power to reach the speed demand and actuates on the accelerator position. The engine maps obtained in the bench tests have been used as inputs to the model to allow the determination of the vehicle performance and emissions during each driving cycle. For each instant, the break mean effective pressure (BMEP) values as well as the engine speed are determined. With these two numbers, it is possible to look-up the values of the inserted parameters inside the maps.

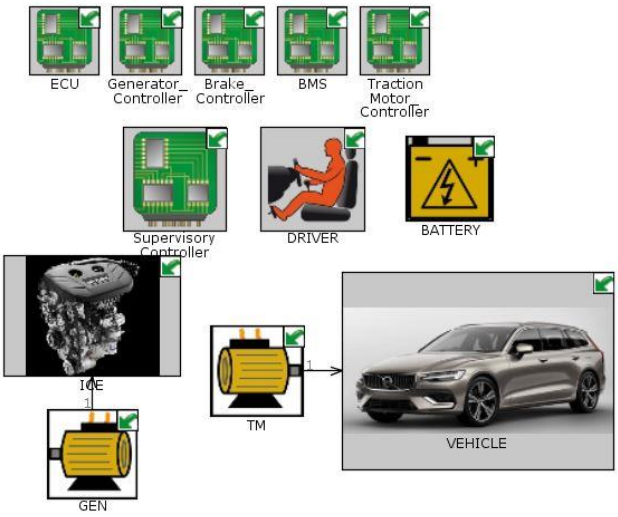

Figure 2. Vehicle model developed in GT- Power® for VOLVO V60.

The instantaneous engine speed values can be directly obtained from the vehicle speed and the respective transmission ratios of each component whilst the BMEP values are determined from the torque values calculated in equation 1. This equation addresses the inertial forces and all the external forces that are acting on the vehicle. On this, I_{trans1} and I_{trans2} present the inertia in the input and output of transmission system, respectively. Likewise, I_{dsh} and I_{axl} are driveshaft and axle moments of inertia. These terms relate the number of axles and inertia of each wheel, adapted to the vehicle characteristics. R_d and R_t are terms of final drive and transmission ratio for each gear. Vehicle speed (ω_{drv}) at the instant of time (t) is directly related to the wheel radius (r_{whl}) and vehicle mass (M_{veh}). For the hybrid powertrain, the battery mass was included in the total M_{veh}. The second term of Equation 1 represents the load induced by a transient gear ratio, where the vehicle object internally creates a transmission model based on the information of vehicle transmission references. External forces on the vehicle are added in the third term as aerodynamic forces (F_d), rolling resistance forces (F_{rol}) and gravity forces (F_{grd}) [40].

$$\tau_{vehicle} = \left[I_{trans1} + \frac{I_{trans2}}{R_t^2} + \frac{I_{dsh}}{R_t^2} + \frac{I_{axl}}{(R_d^2)(R_t^2)} + \frac{(M_{veh})(r_{whl}^2)}{(R_d^2)(R_t^2)}\right]\frac{d\omega_{drv}}{dt} - \left[\frac{I_{trans2}}{R_t^3} + \frac{I_{dsh}}{R_t^3} + \frac{I_{axl}}{(R_d^2)(R_t^3)} + \frac{(M_{veh})(r_{whl}^2)}{(R_d^2)(R_t^3)}\right]\omega_{drv}\frac{dR_t}{dt} + \left[\frac{F_{aer} + F_{rol} + F_{grd}}{R_d R_t}\right]r_{whl} \quad (1)$$

The driving cycles selected to perform the simulations are the NEDC and WLTC. Although the NEDC belongs to an old type approval regulation, simulations have been done to compare the fuel consumption between the PPC series hybrid vehicle (SHV) and the values declared by the manufacturer for the vehicles operating under CDC. Later, simulations have been done under the WLTC to know how the PPC-SHV performs under the conditions proposed in the currently in force homologation cycle. The time-vehicle speed profiles of the NEDC and WLTC cycles are shown in Figure 3.

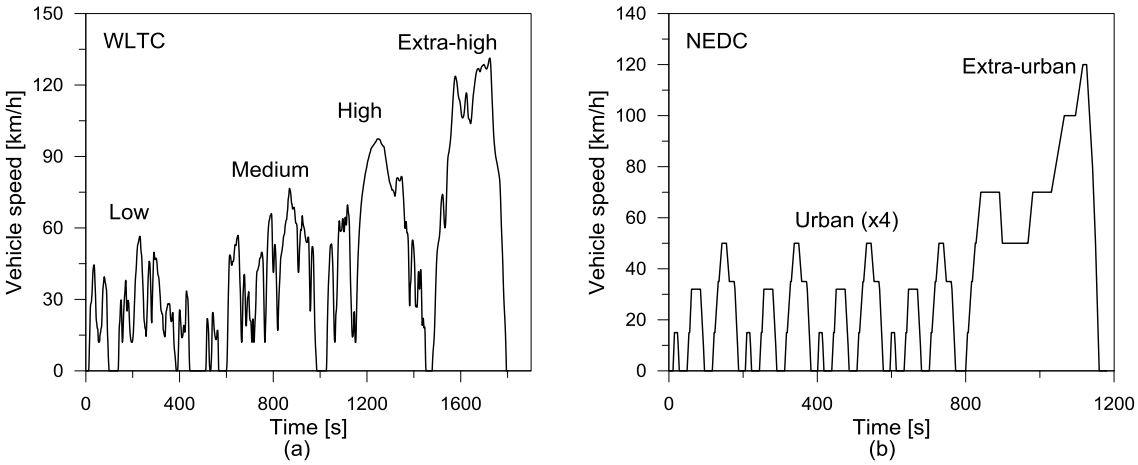

Figure 3. Time-vehicle speed profiles of the WLTC (a) and NEDC (b) cycles.

3. Results and discussion

The results are divided into three subsections. The first one shows the performance and emissions maps obtained in the PPC multi-cylinder engine. The second one describes the battery charging strategy, which is optimized for each vehicle and driving cycle considered in the study. Finally, the performance and emissions of the PPC-SHV concept are evaluated under two driving cycles (NEDC and WLTC) and compared to the homologation values declared by the manufacturer for the vehicles running under CDC.

3.1. Gasoline PPC engine maps

The experimental maps obtained from the test bench are presented from Figure 4 to Figure 6. It is interesting to note that the emissions maps are not optimized, but come from a calibration used for basic studies. As it can be seen, the load range below 4 bar BMEP has not been considered in the study because it presents excessive fuel consumption and emissions values, together with poor combustion controllability and combustion efficiency. In terms of engine speed, the maps were reconstructed excluding conditions with low operating condition density. In this sense, the region below 1300 rpm and above 2400 rpm were discarded because there were not enough data to obtain an accurate interpolation to create the maps. The flexibility of the series hybrid concept allows to overcome this issue excluding conditions where the ICE operation is far from the optimum value, which allows to speed up the optimization process.

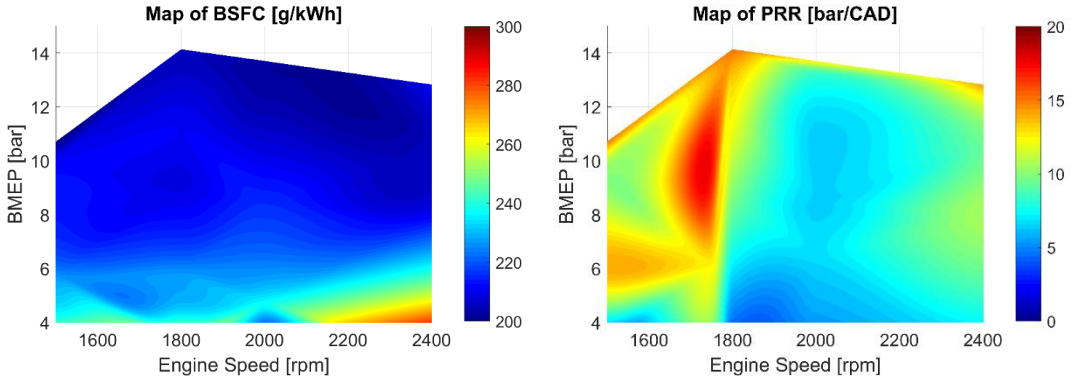

Figure 4. BSFC and PRR for gasoline PPC combustion from experimental results.

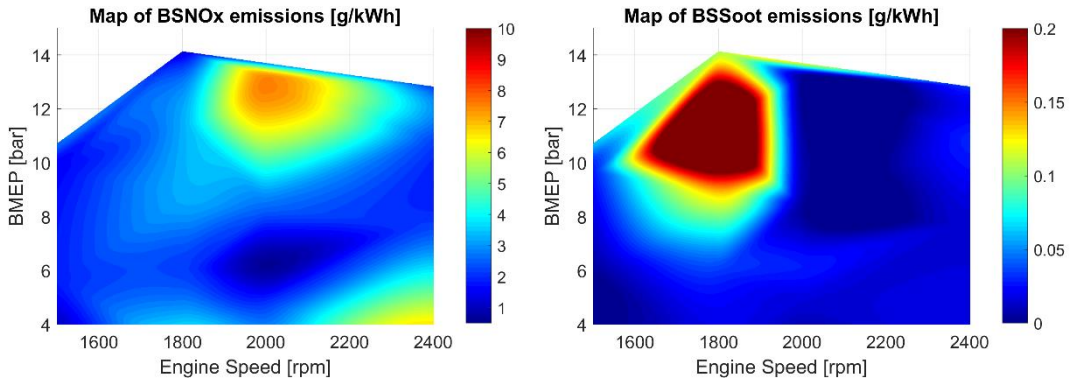

Figure 5. $BSNO_x$ and BSSoot for gasoline PPC combustion from experimental results.

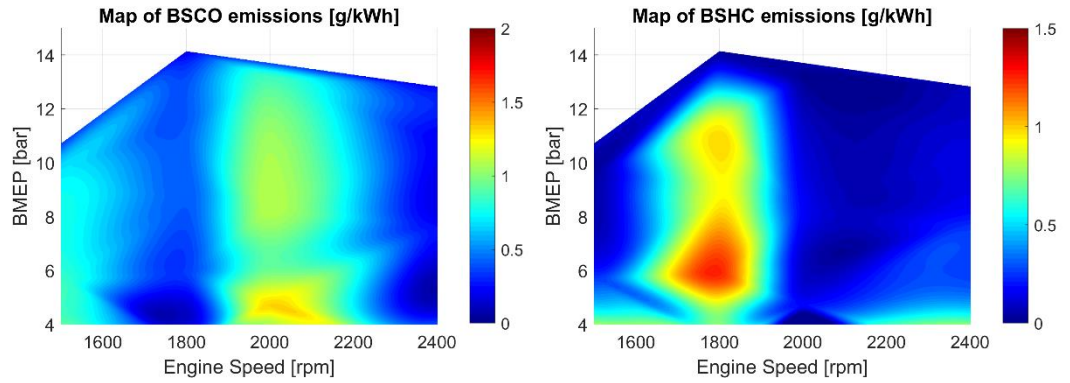

Figure 6. BSCO and BSHC for gasoline PPC combustion from experimental results.

3.2. Battery charging strategy

The rule based control (RBC) used in this research relies on turn on or switch the engine state according to pre-defined objectives. A relevant control parameter considered in the RBC strategy is the battery state of charge (SOC) [41]. As literature demonstrates, the optimum SOC value generally is found in the range 40 %< SOC< 80%. In this sense, SOC< 40% leads to low efficiency of the battery and SOC> 80% is not desired due to the consequent power fade [42]. In this work, the SOC strategy has been fixed as shown in Table 4 considering the optimization performed in a previous research [43]. Once selected, different ICE states (with different power levels) are defined to charge the batteries as needed. The control variable behavior will inform the supervisory control on the real-time battery level, allowing to determine the next decision for the ICE. In this sense, the number of power levels as well as the operating conditions used to charge the batteries will have a direct impact on the performance during the driving cycle. For example, if the ICE runs in a high power operating point, the SOC level will be recovered rapidly. However, it will lead to a great number of on/off states of the ICE, which results in a fuel consumption penalty [43]. Since the driver requested power depends on the drive cycle and vehicle characteristics, these parameters have been optimized independently. Therefore, the next two subsections will focus on the determination of the number of zones and the operating conditions to fully explore the potential of the PPC concept.

Table 4. RBC control strategy.

Transitions	Conditional statement
CD to CS Level 1	State=1 & SOC<0.62
CS Level 1 to CD	State=2 & SOC>0.64
CS Level 1 to CS Level 2	State=2 & SOC<0.60
CS Level 2 to CS Level 1	State=3 & SOC>0.62
CS Level 2 to CS Level 3	State=3 & SOC<0.58
CS Level 3 to CS Level 2	State=4 & SOC>0.60

3.2.1. Influence of the number of power levels

The determination of the number of power levels is a complex problem, since it is dependent on the combination of the operating conditions of each region and the number of starts and stops of the vehicle. Besides, the introduction of additional constraints as for example the final emissions values results in a multi-variable optimization problem. Among the existing methods to solve this problem, the multi-objective Pareto optimization is well addressed in the literature, allowing to determine the optimal solution profile with reasonable computational cost. To allow the use of this method, a sample distribution should be generated addressing the range of values where each factor can be located, and their respective response.

To perform the optimization, the PPC engine map has been divided into different zones of almost equal power, as shown in Figure 7. Then, a design of experiments (DoE) was performed in GT-Power® considering the different factors (engine speed and torque) values and its respective division (one, two, three and four zones). A Latin hypercube DoE method was used to determine the relations between the independent (factor) and dependent (response) variables. This method requires fewer cases than traditional full factorial methods, where all the combinations of the variables should be solved. From this study, the number of cases was incremented according to the number of zones. Thus, the total number of cases for the one, two, three and four zones approaches were 500, 1000, 1500 and 2000, respectively.

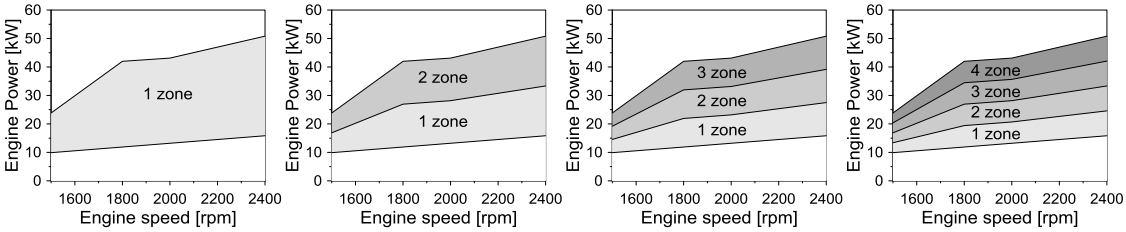

Figure 7. Multi-zone approach to select the optimum number of power levels.

From the DoE results, different response models were adjusted using the Kriging fitting method [44]. The goodness of the fit was assessed by the R^2 values and the graphical dispersion of the observed and predicted values for each dependent factor. Figure 8 illustrates the results obtained for the Volvo XC90 vehicle for the NEDC driving cycle with the engine map divided in three zones. As it can be seen, a proper agreement is verified for the three response parameters, with the R^2 being higher than 83% in all the cases. The same procedure was performed for all conditions obtaining similar results allowing to move for the Pareto optimization.

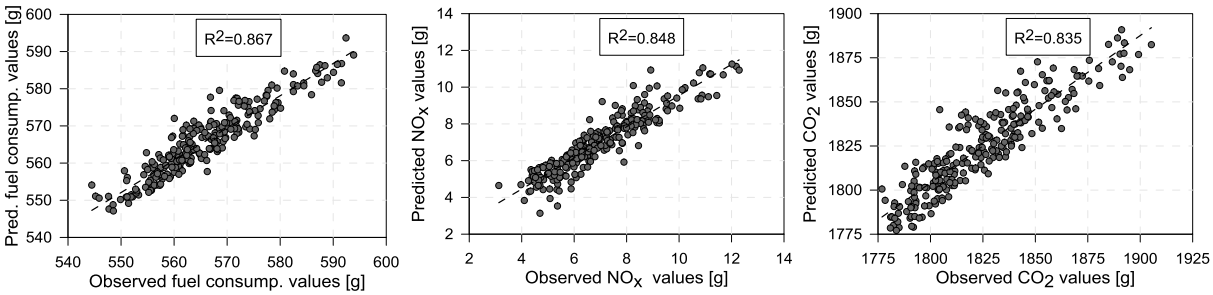

Figure 8. Verification of the predicted results for the adjusted model: comparison for fuel consumption, NO_x and CO_2 values.

Finally, the adjusted models were used to determine the Pareto frontier for each condition that was tested. Figure 9 shows an example obtained from the XC90 model in a one zone division. The circles represent the results from the DoE while the line delimits the Pareto frontier. As it can be seen, the Pareto line follows strictly the points were the minimization is possible. Therefore, for any NOx-fuel consumption criteria, the optimum point will be placed at the Pareto frontier.

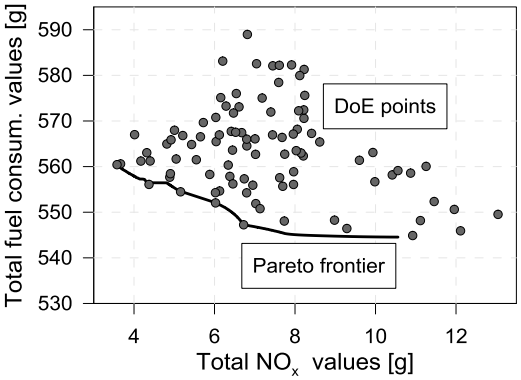

Figure 9. DoE results from the simulation and the respective Pareto frontier. Results obtained for the one zone approach using the XC90 vehicle in the WLTC driving cycle.

One of the requirements for the LTC modes is to achieve low fuel consumption together with reduced NOx emissions. Thus, the criteria imposed for the optimization process aimed to minimize both parameters. The target imposed for the fuel consumption was to reduce it below that declared by the OEM for the conventional diesel powertrain. The target considered for the NOx emissions was the Euro 6 regulation value in the WLTC cycle (0.08 g/km). Figure 10 and 11 present the Pareto results obtained for each driving cycle and the respective number of zones. The vertical dashed lines represent the normative values for NOx while the horizontal ones stand for the fuel consumption obtained from the OEM website [38][39]. The XC90 vehicle is not homologated for WLTC, so that no limit is marked. In any case, the fuel consumption will be higher than for NEDC. The analysis of the figure confirms the well-known trade-off between NOx and fuel consumption independently of the number of zones, from which the reduction in one parameter causes the increase in the other.

From both figures, it is seen that the results provided by the different strategies (number of zones) seems to be affected by the driving cycles and the vehicles characteristics. Figure 10 shows that the higher power demand from the WLTC cycle results in the necessity of using higher ICE power conditions. Besides, the ICE should remain running

for a longer time to recharge the battery. In this sense, the differences among the zones are highlighted, moving the lower fuel consumption values towards the higher number of zones. However, the analysis of the NEDC results has similar values for all the zone divisions. The main reason behind this is the lower vehicle velocities reached during the cycle as well as its lower total duration compared to the WLTC. In this scenario, it is difficult to define the optimal condition.

The effect of the vehicle characteristics can be verified comparing the results from Figure 10 and Figure 11. The first assertion that can be stated is the lower fuel consumption of the V60 vehicle that is attributed to its lower weight and better aerodynamic characteristics. Nonetheless, it is interesting to note the opposite trend for the number of zones compared to the XC90 model. In general, there are improvements from one zone to two zone. However, as the number of zones continues to increase, both fuel consumption and NOx emissions are increased. The V60 vehicle is 25% lighter than the XC90 with a 29% lower effective frontal area (Cd*A), where Cd is the drag coefficient and A is the frontal area, which results in a reduced power demand profile, and therefore leads to lower charge consumption from the batteries and decreased necessity of the ICE. Therefore, the ICE is started fewer times and in lower engine load conditions, hardly reaching charging states higher than the second power level. In this sense, the ICE is forced to run in a condition with high BSFC and emissions values. By contrast, lower number of zones allows to reach higher engine loads, maintaining the engine running for shorter time and improving the vehicle performance.

This brief analysis allowed to verify that dedicated optimizations are needed depending on the driving cycle and vehicles characteristics. Despite of this, the determination of the best number of zones and the operating conditions to be used is not so evident, since it is not clear if a penalization in fuel consumption to reach lower NOx values is advantageous. The methodology proposed to tackle this problem is discussed in the next section.

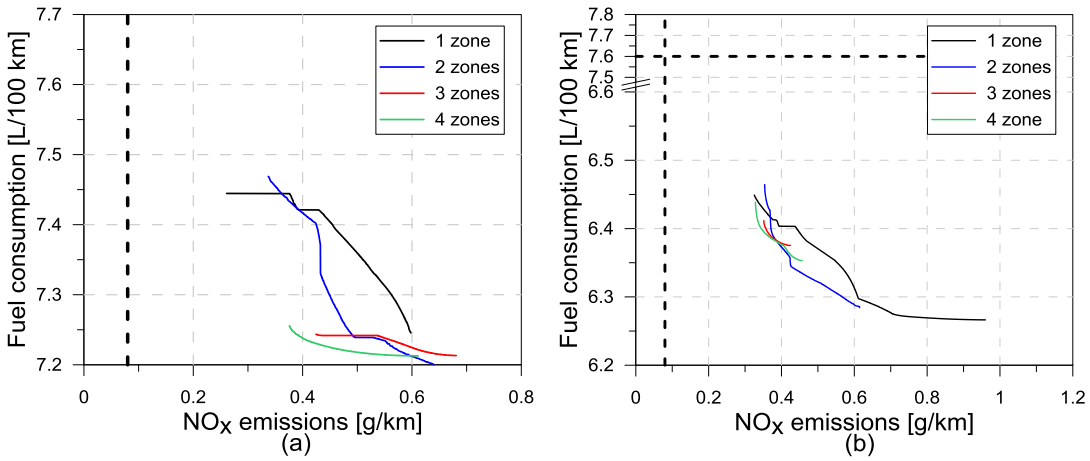

Figure 10. Pareto frontiers for the XC90 vehicle in the WLTC (a) and NEDC (b) for the different number of zones.

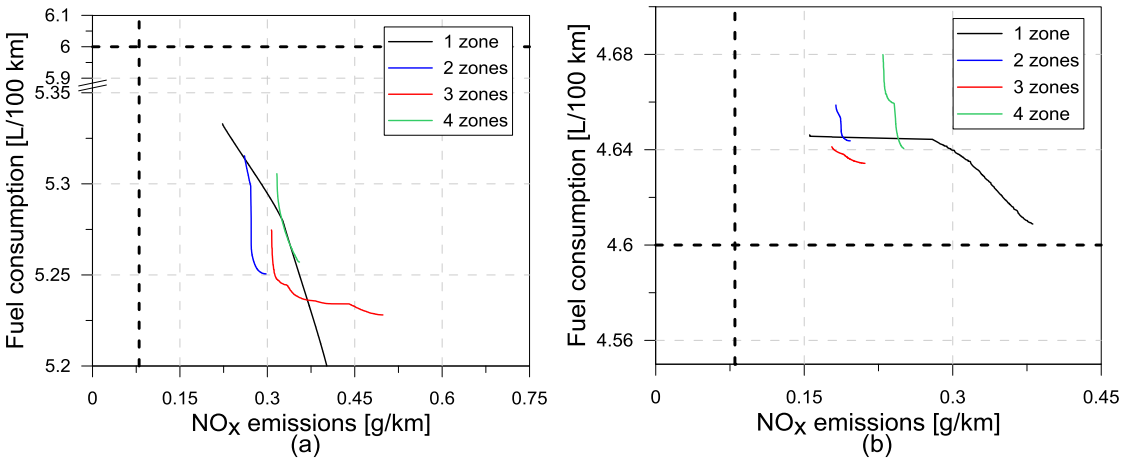

Figure 11. Pareto frontiers for the V60 vehicle in the WLTC (a) and NEDC (b) for the different number of zones.

3.2.2. Determination of the number of power levels and operating conditions

To select the optimum conditions for the different Pareto results obtained in Figure 10 and 11, a methodology was proposed accounting the final urea quantity required to reduce the exhaust NOx to normative standards, as shown in Equation 2 [45]. This value can be summed up with the fuel consumption, resulting in the total fluid consumption (Equation 3). Thus, applying the Equations 2 and 3 for each operating condition verified in the Pareto frontier, it is possible to reduce the problem to a single variable dependency.

$$m_{urea} = \left(NO_x - NO_{x_{Eu6}}\right) * 0.01 * m_{fuel} \ [g] \quad (2)$$

$$m_{total} = m_{fuel} + m_{urea} \quad (3)$$

The results of this process are presented in Figure 12 and Figure 13. As it can be seen, the trend shown in the previous section with respect to the number of zones is maintained. Nonetheless, the reduction to a single variable problem enhances the visualization of the final solution for each case. From Figure 12 it is possible to see that the best solution for the XC90 vehicle, for both cycles, is the four-zone division approach. By contrast, the V60 vehicle has different optimal conditions depending on the driving cycle. For the WLTC case, the two-zone excels as the best solution. However, in the case of NEDC, the three-zone approach was used despite its slightly higher fuel consumption than the one-zone approach. This is justified by the low difference of the fuel consumption values obtained.

The optimum set of operating conditions for each zone is obtained from the searching of the condition where the minimum values of the combined fluid consumption (fuel + urea) is verified. These operating conditions are represented in Figure 14, and will be used as inputs for each model to perform a comparison of the PPC-SHV powertrains versus the diesel commercial ones in terms of performance and emissions.

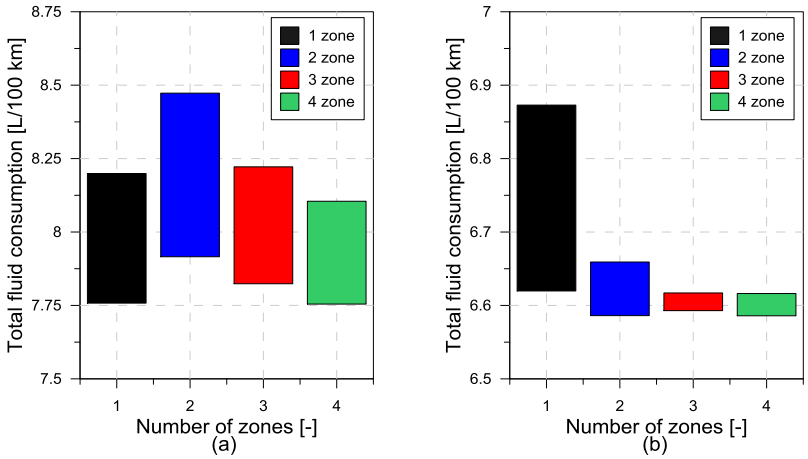

Figure 12. Total fluid consumption range accounting the urea quantity to reduce the NOx levels to the Eu6 limits for the XC90 vehicle in the WLTC (a) and NEDC (b) for the different number of zones.

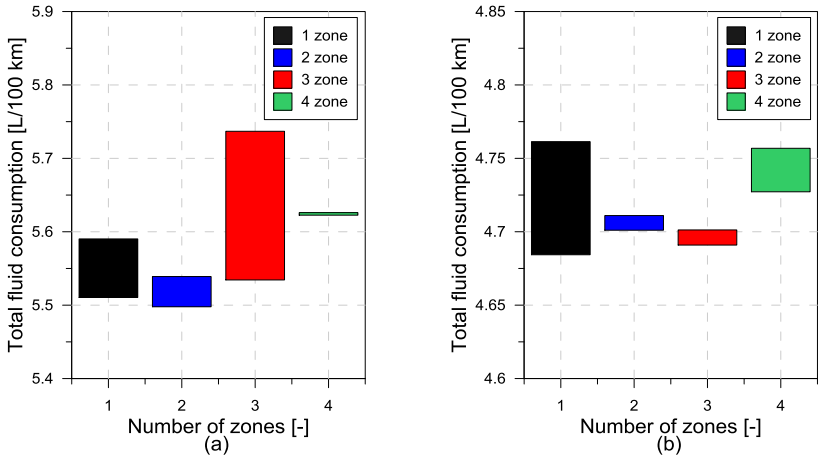

Figure 13. Total fluid consumption range accounting the urea quantity to reduce the NOx levels to the Eu6 limits for the V60 vehicle in the WLTC (a) and NEDC (b) for the different number of zones.

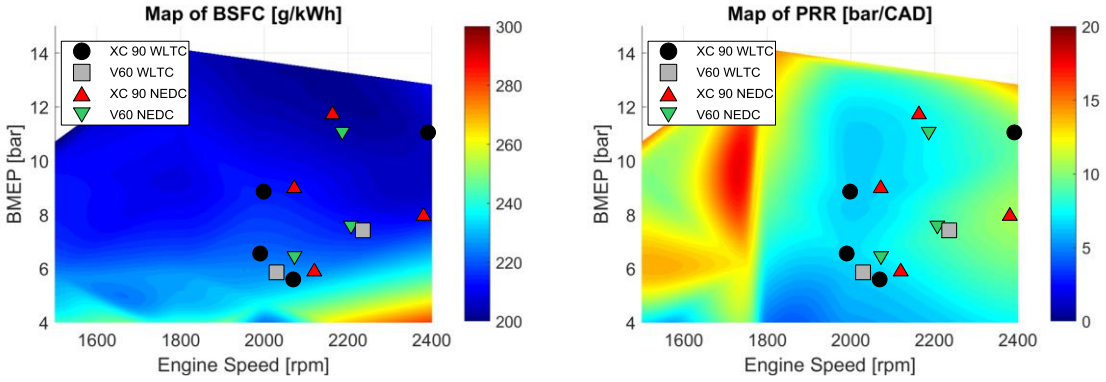

Figure 14. Final operating points selected for the different vehicles and driving cycles after the optimization procedure plotted over the BSFC and PRR maps.

3.3. PPC-SHV performance and emissions

To determine the performance and emissions with the optimum operating conditions and compare them to the OEM powertrains, the GT-power vehicle models were

launched. The results are shown in Figure 15 and Figure 16, which address the ICE requirement during the driving cycle and the impact of it on the instantaneous fuel consumption. Figure 15a summarizes the state of charge behavior and the state occupied by the ICE during the WLTC for both vehicles. As it can be seen, the charging process is generally shorter for the V60 vehicle compared to the XC90. Further, the vehicle can run a longer duration on full electrical mode, i.e., without the necessity of recharging the battery for the first cycle phase despite of its smaller battery capacity. For the following phases, it can be noted that the SOC levels for the V60 vehicle are generally higher than the XC90 vehicle as result of the lower power demand. The combination of the lower charging time and power request leads to lower cumulative fuel consumption for the V60 vehicle as illustrated in Figure 15b. Each step increment in this graph is correlated with the state and the total running time of the ICE and the slope is defined by the total fuel consumption of the charging point.

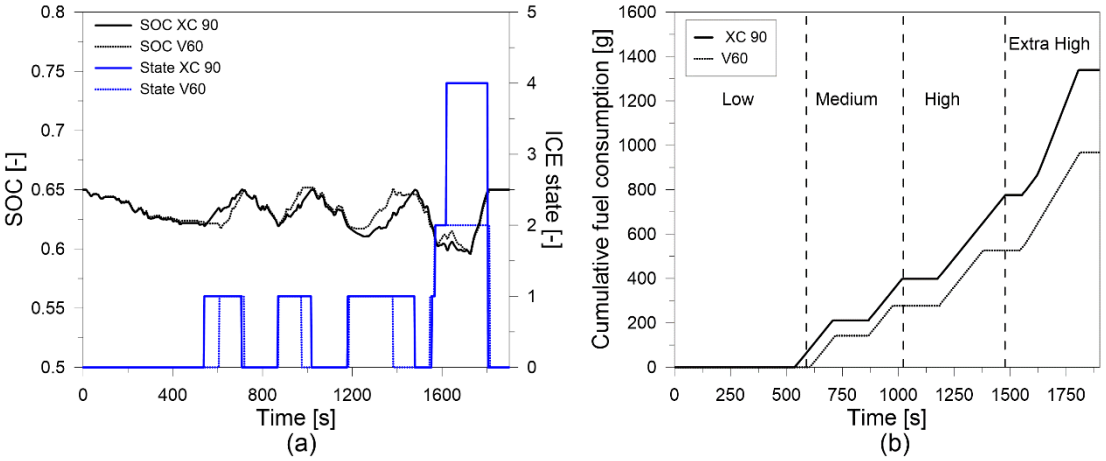

Figure 15. State of charge values and ICE state (a) and the cumulative fuel consumption (b) for the V60 and XC90 vehicles during the WLTC driving cycle.

Figure 16 presents the same analysis for the NEDC driving cycle presented, resulting in similar conclusions. The XC90 model characteristics (weight, effective frontal area,...) are dominant, independently of the driving cycle, resulting in higher fuel consumption. However, it is interesting to note that for the urban part of the NEDC, the fuel consumption difference between the vehicles is much smaller than the one verified at the end of the cycle. The total percentage of fuel consumption from the urban phase for the XC90 is 29% of the total, whilst for the V60 is 33%. Therefore, it can be affirmed that the mass value has lower influence than the vehicle speed, which becomes clear from the motion equation where the mass has linear effect while the vehicle speed is a third power term. In this sense, the hybridization results in better improvements when applied to urban traffic than for highway conditions where the power request is higher and the potential for regenerative braking is reduced.

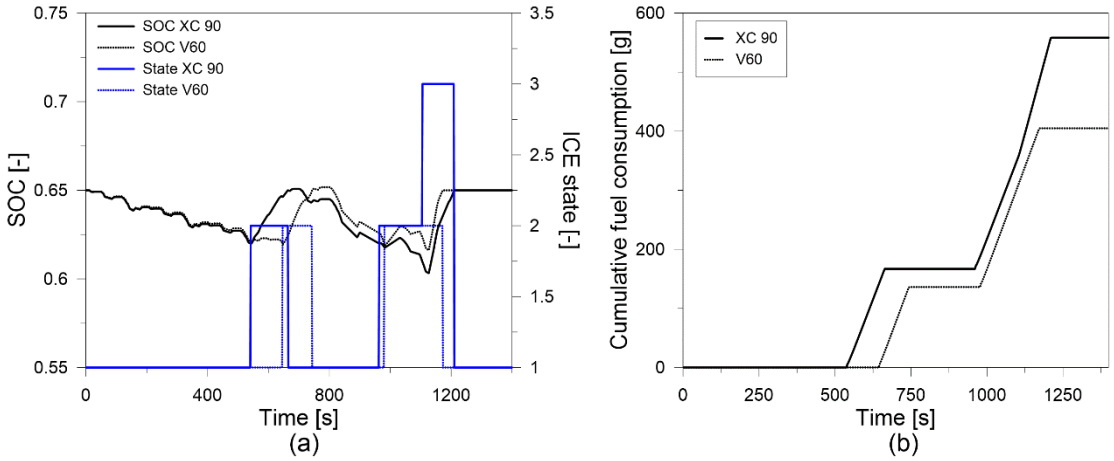

Figure 16. State of charge values and ICE state (a) and the cumulative fuel consumption (b) for the V60 and XC90 vehicles during the NEDC driving cycle.

Table 5 compares the SHV-PPC simulation results to the Euro 6 normative for light-duty vehicles. In addition, a comparison was performed versus the fuel consumption values presented in the OEM website for both vehicles along the NEDC and WLTC. The fuel consumption and CO_2 range shown in Table 5 for the OEM depends on the tires class, where the minimum and maximum values correspond to tires class B and E, respectively.

Despite of the low NO_x values, the PPC concept was not able to reach normative values for this contaminant for any of the conditions tested. Additionally, the HC+NO_x levels also exceed the normative values. From this point of view, an aftertreatment system to reduce HC and NO_x should be required for this concept. Apart from this, satisfactory results were obtained for both soot and fuel consumption for the SHV-PPC concept. Excluding the XC90 vehicle in the WLTC, all the cases tested achieved values of soot lower than the Euro 6 limits. This is an important finding, since it opens the possibility of reducing the DPF size, which will help to reduce the vehicle cost and the parasite losses related to the fuel amount required to regenerate it and the associated back pressure that this device can attribute to the complete system.

Both CO_2 production and fuel consumption values presented reasonable results compared to the ones presented in the OEM website. In general, the values of the hybrid powertrain were able to reach similar or lower values than the lower limit provided for each vehicle. In this sense, it can be concluded that the hybrid powertrain running with PPC combustion is able to achieve similar or better performance than the commercial diesel vehicle with low engine-out emissions.

Finally, Figure 17 shows the total fluid consumption (fuel + urea) needed to ensure that SHV-PPC vehicles fulfill the Euro 6 regulation in terms of NOx emissions. The urea mass needed to be used in the SCR system has been calculated for each case following Equation 2, and taking as NOx target 0.08 g/km. With this, HC+NOx is also fulfilled for the SHV-PPC concept. As the figure shows, the total fluid consumption (fuel + urea) for that SHV-PPC concept is in the range of the fuel consumption (diesel) presented in the OEM website for both diesel vehicles, which does not include the urea consumption in the SCR system.

Table 5. Engine-out emissions for the two vehicles compared to the reference values provided by the manufacturer for the vehicles running under CDC.

Vehicle [-]	Cycle	NOx [g/km]	HC+NO_x [g/km]	CO [g/km]	Soot [g/km]	CO_2 [g/km]	Fuel [L/100 km]
V60 PPC-SHV	NEDC	0.21	0.24	0.13	0.004	118.74	4.66
V60 D3 OEM		-	-	-	-	117-126	4.4-4.6
XC90 PPC-SHV		0.4	0.45	0.13	0.005	163.74	6.42
XC90 OEM		-	-	-	-	158-221	6.0-8.4
V60 PPC-SHV	WLTC	0.29	0.33	0.13	0.004	134.35	5.27
V60 D3 OEM		-	-	-	-	136-157	5.2-6.0
XC90 PPC-SHV		0.46	0.51	0.17	0.007	187.63	7.29
XC90 OEM		-	-	-	-	-	-
Euro 6 limits (WLTC)		0.08	0.17	0.5	0.005	-	-

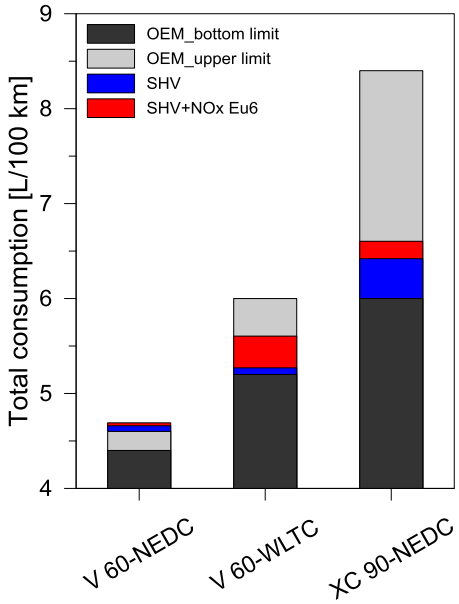

Figure 17. Total consumption for the SHV-PPC vehicles when fulfilling the Euro 6 regulation in terms of NOx emissions compared to the diesel fuel consumption presented in the OEM website.

4. Conclusions

This work investigated the performance of two vehicles adapted to a series hybrid powertrain concept equipped with a 2L Volvo VED-D4 Euro 6 four-cylinder engine running on gasoline PCC combustion mode. A multi-objective Pareto optimization process was carried out to determine the number of ICE operating conditions and the respective values of engine speed and BMEP to minimize both fuel consumption and NOx emissions. From this study, it was found that:

- The number of ICE operating points needed to charge the batteries is dependent on the driving cycle and the vehicle class. For heavy vehicles as the XC90, the power request profile results in a better utilization of higher engine loads whilst for the V60, low engine load conditions are able to recharge the batteries.

- To determine the operating conditions, the problem should be reduced to a single variable. For this, a cost function based on the total NOx amount to be converted in order to reach the Euro 6 normative was successfully implemented allowing to determine the best ICE operating conditions.

The analysis of the instantaneous fuel consumption traces allowed to verify the potential of the hybridization in urban traffic conditions. In such conditions, the regenerative braking and lower power request results in higher energy savings. In addition, the difference between the two vehicles is lower for this phase of the cycle than for the highway, indicating that the vehicle velocity plays a fundamental role on the hybrid performance.

Finally, the final driving cycle results enabled the direct comparison versus the values obtained with the diesel commercial vehicles. In general, both PPC hybrid powertrains were able to reach similar fuel consumption values in the middle of the range to those obtained by the diesel commercial vehicles (from -22% to +7% depending on the vehicle model and driving cycle). In this sense, it is expected that fuel consumption benefits can be improved in the future by optimizing the PPC combustion maps. Regarding the engine-out emissions, the HC and NOx levels were higher than the Euro 6 limits whilst soot and CO were able to fulfill their normative limits for almost all conditions. This results show the potential to minimize the aftertreatment requirement versus a conventional diesel vehicle, proving the PPC-SHV concept to be an alternative to the conventional powertrains enabling the reduction of the tailpipe emissions values without penalizing the performance and CO_2 values.

Acknowledgments

The authors gratefully acknowledge FEDER and Spanish Ministerio de Economía y Competitividad for partially supporting this research through TRANCO project (TRA2017-87694-R). The authors also gratefully acknowledge the KCFP Engine Research Center (Swedish Energy Agency grant number 22485-4) for partial support of this research.

References

[1] Araghi Y, Kroesen M, Van Wee B. Identifying reasons for historic car ownership and use and policy implications: An explorative latent class analysis. Transport Policy, Volume 56, May 2017, Pages 12-18.
[2] Kalghatgi. Is it really the end of internal combustion engines and petroleum in transport? Applied Energy, Volume 225, September 2018, Pages 965-974.
[3] Singh S, Kennedy C. Estimating future energy use and CO2 emissions of the world's cities. Environmental Pollution, Volume 203, August 2015, Pages 271-278.
[4] Commission Regulation (EC) No 692/2008 of 18 July 2008 implementing and amending Regulation (EC) No 715/2007 of the European Parliament and of the Council on type-approval of motor vehicles with respect to emissions from light passenger and commercial vehicles (Euro 5 and Euro 6) and on access to vehicle repair and maintenance information. Off. J. Eur. Union L199, 1-136. European Commission, 2008.
[5] Posada F, Chambliss S, Blumberg K. Costs of emission reduction technologies for heavy-duty diesel vehicles. ICCT White paper 2016.

[6] Jiaqiang E, Zuo W, Gao J, Peng Q, Zhang Z, Hieu P. Effect analysis on pressure drop of the continuous regeneration-diesel particulate filter based on NO2 assisted regeneration. Applied Thermal Engineering, Volume 100, 2016, Pages 356-366.
[7] García-Valladolid P, Tunestal P, Monsalve-Serrano J, García A, Hyvönen J. Impact of diesel pilot distribution on the ignition process of a dual fuel medium speed marine engine. Energy Conversion and Management, Volume 149, 1 Oct 2017, Pages 192-205.
[8] Olmeda P, García A, Monsalve-Serrano J, Sari R. Experimental investigation on RCCI heat transfer in a light-duty diesel engine with different fuels: Comparison versus conventional diesel combustion. Applied Thermal Engineering, Volume 144, November 2018, Pages 424-436.
[9] Yao M, Zheng Z, Liu H. Progress and recent trends in homogeneous charge compression ignition (HCCI) engines. Progress in Energy and Combustion Science, Volume 35, Issue 5, 2009, Pages 398-437.
[10] Maurya R, Agarwal A. Experimental investigation on the effect of intake air temperature and air–fuel ratio on cycle-to-cycle variations of HCCI combustion and performance parameters. Applied Energy 2011, 88, 1153–63.
[11] Singh A, Agarwal A. Combustion characteristics of diesel HCCI engine: an experimental investigation using external mixture formation technique. Appl Energy 2012, 99, 116–25.
[12] Saxena S, Bedoya I. Fundamental phenomena affecting low temperature combustion and HCCI engines, high load limits and strategies for extending these limits. Progress in Energy and Combustion Science, Volume 39, Issue 5, 2013, Pages 457-488.
[13] Komninos N. Assessing the effect of mass transfer on the formation of HC and CO emissions in HCCI engines, using a multi-zone model. Energy Conversion and Management, Volume 50, Issue 5, 2009, Pages 1192-1201.
[14] Inagaki K, Fuyuto T, Nishikawa K, Nakakita K, Sakata I. “Dual-Fuel PCI Combustion Controlled by In-Cylinder Stratification of Ignitability,” SAE Technical Paper 2006-01-0028, 2006.
[15] Molina S, García A, Monsalve-Serrano J, Estepa D. Miller cycle for improved efficiency, load range and emissions in a heavy-duty engine running under reactivity controlled compression ignition combustion. Applied Thermal Engineering, Volume 136, 2018, Pages 161-168.
[16] Benajes J, García A, Monsalve-Serrano J, Boronat V. Gaseous emissions and particle size distribution of dual-mode dual-fuel diesel-gasoline concept from low to full load. Applied Thermal Engineering, Volume 120, 2017, Pages 138-149.
[17] Li Y, Jia M, Chang Y, Xie M, Reitz R. Towards a comprehensive understanding of the influence of fuel properties on the combustion characteristics of a RCCI (reactivity controlled compression ignition) engine. Energy, Volume 99, 2016, Pages 69-82.
[18] Benajes J, García A, Monsalve-Serrano J, Balloul I, Pradel G. Evaluating the reactivity controlled compression ignition operating range limits in a high-compression ratio medium-duty diesel engine fueled with biodiesel and ethanol. International Journal of Engine Research, Volume 18 (1-2), Pages 66-80, 2017.

[19] Qian Y, Ouyang L, Wang X, Zhu L, Lu X. Experimental studies on combustion and emissions of RCCI fueled with n-heptane/alcohols fuels. Fuel, Volume 162, 2015, Pages 239-250.
[20] Benajes J, García A, Monsalve-Serrano J, Boronat V. Dual-Fuel Combustion for Future Clean and Efficient Compression Ignition Engines. Applied Sciences 7(1):36, 2017.
[21] Zhou D, Yang W, An H, Li J. Application of CFD-chemical kinetics approach in detecting RCCI engine knocking fuelled with biodiesel/methanol. Applied Energy, Volume 145, 2015, Pages 255-264
[22] García A, Monsalve-Serrano J, Rückert Roso V, Santos Martins M. Evaluating the emissions and performance of two dual-mode RCCI combustion strategies under the World Harmonized Vehicle Cycle (WHVC). Energy Conversion and Management, Volume 149, 2017, Pages 263-274.
[23] Benajes J, García A, Monsalve-Serrano J, Boronat V. An investigation on the particulate number and size distributions over the whole engine map from an optimized combustion strategy combining RCCI and dual-fuel diesel-gasoline. Energy Conversion and Management, Volume 140, 2017, Pages 98-108.
[24] Wang Y, Yao M, Li T, Zhang W, Zheng Z. A parametric study for enabling reactivity controlled compression ignition (RCCI) operation in diesel engines at various engine loads. Applied Energy, Volume 175, 2016, Pages 389-402.
[25] Benajes J, García A, Monsalve-Serrano J, Sari R. Evaluating the Efficiency of a Conventional Diesel Oxidation Catalyst for Dual-Fuel RCCI Diesel-Gasoline Combustion. SAE Technical Paper, 2018-01-1729, 2018, doi: 10.4271/2018-01-1729.
[26] Benajes J, García A, Monsalve-Serrano J, Sari R. Experimental investigation on the efficiency of a diesel oxidation catalyst in a medium-duty multi-cylinder RCCI engine. Energy Conversion and Management, Volume 176, November 2018, Pages 1-10.
[27] García A, Piqueras P, Monsalve-Serrano J, Sari R. Sizing a conventional diesel oxidation catalyst to be used for RCCI combustion under real driving conditions. Applied Thermal Engineering, Volume 140, July 2018, Pages 62-72.
[28] Yang Y, Dec J, Dronniou N, Sjöberg M. Tailoring HCCI heat-release rates with partial fuel stratification: Comparison of two-stage and single-stage-ignition fuels. Proceedings of the Combustion Institute, Volume 33 (2), pp. 3047-3055, 2011.
[29] Belgiorno B, Dimitrakopoulos N, Di Blasio G, Beatrice C, Tunestal P, Tunér M. Parametric Analysis of the Effect of Pilot Quantity, Combustion Phasing and EGR on Efficiencies of a Gasoline PPC Light-Duty Engine. SAE Technical paper, 2017-24-0084 2017, doi: 10.4271/2017-24-0084.
[30] Belgiorno B, Dimitrakopoulos N, Di Blasio G, Beatrice C, Tunestal P, Tunér M. Effect of the engine calibration parameters on gasoline partially premixed combustion performance and emissions compared to conventional diesel combustion in a light-duty Euro 6 engine. Applied Energy, Volume 228, October 2018, Pager 2221-2234.
[31] Kalghatgi GT. Auto-ignition quality of practical fuels and implications for fuel requirements of future SI and HCCI engines. SAE paper 2005-01-0239, 2005
[32] Benajes J, Molina S, García A, Monsalve-Serrano J, Durrett R. Conceptual model description of the double injection strategy applied to the gasoline partially premixed compression ignition combustion concept with spark assistance. Applied Energy, Volume 129, 2014, Pages 1-9.

[33] Benajes J, Molina S, García A, Monsalve-Serrano J, Durrett R. Performance and engine-out emissions evaluation of the double injection strategy applied to the gasoline partially premixed compression ignition spark assisted combustion concept. Applied Energy, Volume 134, 2014, Pages 90-101.
[34] Solouk a, Tripp J, Shakiba-Herfeh M, Shahbakhti M, Fuel consumption assessment of a multi-mode low temperature combustion engine as range extender for an electric vehicle. Energy Conversion and Management, Volume 148, September 2017, Pages 1478-1496,
[35] Thiel C, Perujo A, Mercier A. Cost and CO_2 aspects of future vehicle options in Europe under new energy policy scenarios. Energy Policy, Volume 38, August 2010, Pages 7142-7151.
[36] Heywood J. Internal combustion engine fundamentals. McGraw-Hill; 1988.
[37] Shen M, Tuner M, Johansson B, Cannella W. Effects of egr and intake pressure on ppc of conventional diesel, gasoline and ethanol in a heavy duty diesel engine. SAE Int 2013. https://doi.org/10.4271/2013-01-2702.
[38] https://www.media.volvocars.com/global/en-gb/models/new-v60/2019/specifications (accessed in 25/09/2018).
[39] https://www.media.volvocars.com/global/en-gb/models/xc90/2019/specifications (accessed in 25/09/2018).
[40] Gamma Technologies: Vehicle Driveline and HEV Application Manual. 2018.
[41] Panday A, Om Bansal H. Hybrid Electric vehicle Performance Analysis under Various Temperature Conditions. Energy Procedia, Volume 75, 2015, Pages 1962-1967.
[42] Forman J C, Moura S J, Stein J L, Fathy H K. Optimal experimental design for modeling battery degradation. ASME Dynamic Systems and Control Conference, October 2012.
[43] Benajes J, García A, Monsalve-Serrano J, Sari R. Potential of RCCI Series Hybrid Vehicle Architecture to Meet the Future CO2 Targets with Low Engine-Out Emissions. Applied Sciences, Volume 6, August 2018.
[44] Oliver M, Webster R (1990): Kriging: a method of interpolation for geographical information systems, International Journal of Geographical Information Systems, 4:3, 313-332.
[45] Commission Regulation (EC) No 692/2008 of 18 July 2008 implementing and amending Regulation (EC) No 715/2007 of the European Parliament and of the Council on type-approval of motor vehicles with respect to emissions from light passenger and commercial vehicles (Euro 5 and Euro 6) and on access to vehicle repair and maintenance information. Off. J. Eur. Union L199, 1-136. European Commission, 2008.

Abbreviations

BMEP: Break Mean Effective Pressure

BSFC: Break Specific Fuel Consumption

CD: Charge Depleting

CDC: Conventional Diesel Combustion

CO: Carbon Monoxide

CS: Charge Sustaining

DME: Di-Methyl Ether

DOE: Design of Experiments

DOC: Diesel Oxidation Catalyst

DPF: Diesel Particulate Filter

EGR: Exhaust Gas Recirculation

HC: Hydro Carbons

HCCI: Homogeneous Charge Compression Ignition

HR: Heat Release

HRR: Heat Release Rate

HRF: High Reactivity Fuel

ICE: Internal Combustion Engine

LRF: Low Reactivity Fuel

LTC: Low Temperature Combustion

MON: Motor Octane Number

NEDC: New European Driving Cycle

NOx: Nitrogen Oxides

OEM: Original Equipment Manufacturer

ON: Octane Number

PCI: Premixed Compression Ignition

PPC: Partially Premixed Combustion

RBC: Rule Based Control

RCCI: Reactivity Controlled Compression Ignition

RON: Research Octane Number

SCR: Selective Catalytic Reduction

SHV: Series Hybrid Vehicle

SOC: State of Charge

WLTC: Worldwide harmonized Light vehicles Test Cycle